Atmos. Chem. Phys. Discuss., doi:10.5194/acp-2016-370, 2016
Manuscript under review for journal Atmos. Chem. Phys.
Published: 25 May 2016

Atmospheric Chemistry and Physics Discussions

Current and future levels of mercury atmospheric pollution on global scale

Jozef M. Pacyna[1,6], Oleg Travnikov[2], Francesco De Simone[3], Ian M. Hedgecock[3], Kyrre Sundseth[1], Elisabeth G. Pacyna[1], Frits Steenhuisen[4], Nicola Pirrone[5], John Munthe[7] and Karin Kindbom[7]

[1]NILU – Norwegian Institute for Air Research, Instituttveien 18, PO Box 100, NO-2027 Kjeller, Norway
[2]Meteorological Synthesizing Centre - East of EMEP, 2nd Roshchinsky proezd, 8/5, office 207, 115419 Moscow, Russian Federation
[3]CNR – Institute of Atmospheric Pollution Research, Division of Rende, UNICAL-Polifunzionalie, Rende 87036, Italy
[4]University of Groningen, Arctic Centre, Aweg 30, 9718 CW Groningen, The Netherlands
[5]CNR – Institute of Atmospheric Pollution Research, Area della Ricerca Roma 1, Via Salaria Km 29,300, 00015 Monterotondo (Rome), Italy
[6]Gdansk University of Technology (GUT), Chemical Faculty, 11/12 G, Narutowicza Str., PL-80-952 Gdansk Wrzeszcz, Poland
[7]IVL Swedish Environmental Research Institute, PO Box 53201, 400 14 Gothenburg, Sweden

Correspondence to: Jozef M. Pacyna (jp@nilu.no)

Abstract. An assessment of current and future emissions, air concentrations and atmospheric deposition of mercury world-wide are presented on the basis of results obtained during the performance of the EU GMOS (Global Mercury Observation System) project. Emission estimates for mercury were prepared with the main goal of applying them in models to assess current (2013) and future (2035) air concentrations and atmospheric deposition of this contaminant. The artisanal and small-scale gold mining, as well as combustion of fossil fuels (mainly coal) for energy and heat production in power plants and in industrial and residential boilers are the major anthropogenic sources of Hg emissions to the atmosphere at present. These sources account for about 37% and 25% of the total anthropogenic Hg emissions globally, estimated to be about 2000 tonnes. The emissions in Asian countries, particularly in China and India dominate the total emissions of Hg. The current estimate of mercury emissions from natural processes (primary mercury emissions and re-emissions), including mercury depletion events, were estimated to be 5207 tonnes per year which represent nearly 70% of the global mercury emission budget. Oceans are the most important sources (36%) followed by biomass burning (9%). A comparison of the 2035 anthropogenic emissions estimated for 3 different scenarios with current anthriopogenic emissions indicates a reduction of these emissions in 2035 up to 85 % for the best case scenario.

Two global chemical transport models (GLEMOS and ECHMERIT) have been used for the evaluation of future Hg pollution levels considering future emission scenarios. Projections of future changes in Hg deposition on a global scale simulated by these models for three anthropogenic emissions scenarios of 2035 indicate a decrease of up to 50 % deposition in the Northern Hemisphere and up to 35 % in Southern Hemisphere for the best case scenario.

Atmos. Chem. Phys. Discuss., doi:10.5194/acp-2016-370, 2016
Manuscript under review for journal Atmos. Chem. Phys.
Published: 25 May 2016

The EU GMOS project has proved to be a very important research instrument for supporting, first the scientific justification for the Minamata Convention, and then monitoring of the implementation of targets of this Convention, as well as, the EU Mercury Strategy. This project provided the state-of-the art with regard to the development of the latest emission inventories for mercury, future emission scenarios, dispersion modelling of atmospheric Hg on global and regional scale, and source – receptor techniques for Hg emission apportionment on a global scale.

Key words:

Mercury, anthropogenic emission, natural emission, emission inventory, transport model, atmospheric deposition, source-receptor apportionment.

1 Introduction

Mercury has been recognized as a toxic, persistent, and mobile contaminant. This contaminant does not degrade easily in the environment and it is mobile because of the volatility of the element and several of its compounds. It has the ability to be transported within air masses over very long distances. High doses of organic compounds of mercury, particularly methylmercury (MeHg,) can be fatal to humans but even relatively low doses can seriously affect the human nervous system. Mercury has been also linked with possible harmful effects on the cardiovascular, immune and reproductive systems. Methylmercury passes through both the placenta and the blood-brain barrier, so exposure of women of child-bearing age and of children to methylmercury is of greatest concern. Consequently, several studies have been conducted on the behavior of mercury in the environment and its environmental, human health, and economic consequences (e.g., Ambio, 2007; Lindberg et al 2002; Pacyna et al., 2010, Sundseth et al., 2010: Sundseth et al., 2015; Gustin et al., 2016).

The major conclusion drawn from recent studies on the impacts of mercury on the environment and human health is that there is a need for international action to reduce emissions of and human exposure to mercury on a regional and global scale. The EU Mercury Strategy was launched in 2005 (and reviewed in 2010) to support and encourage European-wide action on mercury reduction and to ban its use. The EU's Mercury Strategy provided a comprehensive plan incorporating actions addressing mercury pollution both in the EU and globally. It identified a variety of actions to decrease mercury emissions, cut supply, reduce demand and protect against exposure, especially to methylmercury found in fish. The strategy resulted in restrictions on the sale of measuring devices containing mercury, a ban on exports of mercury from the EU (that recently came into force), and new rules on safe storage. An overview of EU regulations and directives on mercury emissions can be found in Sundseth (2012).

In 2013 under the United Nations Environment Programme (UNEP), countries signed the Minamata Convention on Mercury, a legally binding agreement intended “to protect human health and the environment from anthropogenic emissions and releases of mercury and mercury compounds” (Article 1 in UNEP 2013). The Convention builds upon scientific

Atmos. Chem. Phys. Discuss., doi:10.5194/acp-2016-370, 2016
Manuscript under review for journal Atmos. Chem. Phys.
Published: 25 May 2016

Atmospheric Chemistry and Physics Discussions

knowledge of global sources and supply, sinks, and reservoirs of Hg, coupled to linkages with human and wildlife exposures and related health impacts.

Implementation of targets of the Minamata Convention, the EU Mercury Strategy and other policies aiming at the reduction of Hg emissions and their impacts requires an accurate assessment of Hg behavior in the environment. It became clear that the atmosphere is the major transport pathway for the global distribution of Hg. A part of the emissions entering the atmosphere is locally deposited to aquatic and terrestrial ecosystems. Another part is transported with air masses in directions dependent on many factors, including wind direction and speed, and mercury behavior during this transport. As a consequence, mercury emitted in one part of the world can be transported to another. However, the spatial distribution of mercury concentrations and deposition is quite uneven. The question arises from decision makers whether analytical tools are now available to accurately assess these source- receptor relationships for mercury. Are the models and other statistical methods good enough to convincingly conclude on sources of emissions for mercury monitored at a given site? If yes, are they good enough for such analysis everywhere in the globe, or maybe only in Europe or North America? If not, what are the main obstacles preventing such an analysis? A lack of answers or incomplete answers to the above mentioned questions result in communication problems between researchers and the decision makers responsible for proposing environmental strategies and implementation plans within the Minamata Convention and other international and regional agreements on the reduction of mercury pollution of the environment.

Launched in November 2010, the EU-funded Global mercury Observation System (GMOS) (www.gmos.eu) has undertaken studies addressing the above mentioned questions concerning source – receptor relationships for mercury. Both, monitoring and model simulations were used for this purpose. The main results from the assessment of current and future emissions, air concentrations and atmospheric deposition of mercury world-wide are presented in this paper.

2 Assessment of emissions and future emission scenarios

Emission estimates for mercury were prepared with the main goal of applying them in models to assess current (2013) and future (2035) air concentrations and atmospheric deposition of this contaminant.

2.1 Methodology

The approach to estimate the current and future Hg emissions consisted of three steps; i) compilation of the current and future activity data, such as data on consumption of fuels and raw materials and production of industrial goods, ii) link these activities to a compilation of unabated emission factors (UEFs) to derive estimates on unabated emissions to air, and iii) characterization of the effectiveness of air pollution control devices (APCDs) or waste practices and their current and future degree of application. The conceptual approach used to produce the scenario inventories is based on the methodology developed in AMAP/UNEP (2013), illustrated in Fig. 1, below.

Atmos. Chem. Phys. Discuss., doi:10.5194/acp-2016-370, 2016
Manuscript under review for journal Atmos. Chem. Phys.
Published: 25 May 2016

Atmospheric Chemistry and Physics Discussions

Fig. 1 here

Being consistent with the methodology developed in AMAP/UNEP (2013), the methodology for estimating future Hg emissions includes the development of two database modules, one on the projected future activities and the other one on emission factors and emission reduction technology employed in the future for different countries.

2.2 Database on activities

Sector activities relate to national statistics on consumption or production of industrial raw materials or outputs for each Hg-emitting economic sector. Current (2010) statistical data presented in AMAP/UNEP (2013) were collected from national and international experts, international organizations (such as UNEP and IEA), industry associations and national bureaus (such as the US Geological Survey - USGS). These current statistics were then linked to future projections, supported by several official databases, such as the International Energy Agency (IEA), the International Monetary Fund (IMF), the World Bank (WB), the Organisation for Economic Co- operation and Development (OECD) and the United Nations (UN). Future activity data for the year 2035 were estimated and compiled from three data sources/ methodologies in the following way:

- to estimate future energy consumption and production data, the UNEP 2010 estimates were projected in line with the International Energy Agency (IEA) projections presented in the World Energy Outlook (WEO) 2012,
- to estimate the various country- specific industrial goods consumption and production data in the future, a methodology consisting of a year 2035 forecast was developed based on a simple regression model that relates resource consumption/production to a nation`s Gross Domestic Product (GDP) per capita (representing the market value of all goods and services produced within a country). The model fitted a straight line through the set of points for all counties in which the slope represented the correlation between national GDP per capita PPP (purchase power parity) and national annual production of industrial goods. The future projection was then estimated on the basis of forecasting industrial consumption/production on the expectations of development of GDP per capita PPP in various countries, based on the OECD database on previous and current GDP per capita PPP as well as the IMF future expectations on GDP per capita PPP,
- to estimate the intentional use of Hg in products, an assumption on voluntary future reductions was made. Assumptions on various degrees of reduced use of Hg in products are based on previously observed trends for different regions (AMAP, 2010) in combination with expectations on implementation of the Minamata Convention. Regional consumption figures used as the basis for the scenarios are presented in UNEP/AMAP (2013), distributed between countries in each region, based on GDP PPP comparisons.

Atmos. Chem. Phys. Discuss., doi:10.5194/acp-2016-370, 2016
Manuscript under review for journal Atmos. Chem. Phys.
Published: 25 May 2016

Atmospheric Chemistry and Physics Discussions

2.3 Database on emission factors and future emission reduction technology employed

Country- specific unabated emission factors based on expert evaluation and national data were compiled for AMAP/UNEP (2013). Furthermore, using the method developed in AMAP/UNEP (2013), countries have been assigned to 5 groupings representing different levels of technological implementation (technological profiles) of APCDs. These technologies were characterized by their effectiveness of emission control and degree of application in a given industrial technology. Various assumptions on future application were then made by assuming various step-by-step technology improvements for each country compared to the 2010 situation. The technological profiles were then applied to the 2010 uncontrolled emission estimates and the future activities for the countries/ sectors, resulting in national sector-estimates of unintentional Hg emissions to the atmosphere.

Hg emissions to air from wastes associated with sectors using Hg intentionally for the various countries were based on world region consumption data as well as on assumptions regarding rates of breakage, degrees of waste handling/incineration and suitable emission factors. The consumption data were distributed between the countries based on GDP per capita PPPs, see Annex 3 and 4 in UNEP/AMAP (2013). Four different categories of waste management practices (such as waste recycling, controlled- or uncontrolled incineration and land-filling) were assigned to individual countries, based on GDP PPP, where group 1 is the most advanced while group 4 has the least developed practices. Various assumptions on future projections on consumption, as well as the waste management practices and emission factors constituted the emission scenario from sectors using Hg intentionally. Emissions from use of Hg in Artisanal Gold Mining was estimated based on consumption patterns and assumed emissions to air from different methods employed in different regions, see Annex 2 in UNEP/AMAP (2013).

2.4 Definition of emission scenarios

Three main sets of projections were chosen as the basis for compiling future (2035) Hg emissions:

The Current Policies Scenario (CPS): The scenario assumes that governmental policies and measures existing in 2010 are adopted, including those that have not been fully implemented. This includes the implementation of traditional APCDs, but also those measures designed to prevent climate change as well as address other environmental problems through energy efficiency and switching to lower carbon fuels. The WEO CPS for 2035 was adopted for the energy sector. The scenario does not include likely future policy initiatives. Thus, it does not forecast the future situation, but it gives rather a baseline vision on energy, industrial goods and products consumption and production as well as the use of APCDs and waste management practices that are likely to change given no additional effort with regard to policy making.

The New Policies Scenario (NPS): The scenario assumes that policy commitments and plans announced by countries worldwide to reduce greenhouse gas emissions, as well as phase out fossil- energy subsidies, are fully implemented. National climate commitments relate to the period of 2020, but additional measures are assumed to be implemented at the 2010 to 2020 pace for the period 2020 to 2035. Future consumption/production of industrial goods is assumed to be at the same level

Atmos. Chem. Phys. Discuss., doi:10.5194/acp-2016-370, 2016
Manuscript under review for journal Atmos. Chem. Phys.
Published: 25 May 2016

Atmospheric Chemistry and Physics Discussions

as in the CPS, while the use of Hg in products is assumed to be reduced by 70% in 2035 compared to the 2010 situation as a result of the assumptions within the Minamata Convention, Annex A. It is furthermore assumed that all countries will move one step up into more advanced waste practices compared to 2010.

The 450 [ppm] Scenario (450ppm): The scenario sets out a target of all counties reaching the highest feasible/available reduction efficiency in each emission sector. The scenario is not a very realistic one, but it illustrates the maximum possible Hg emission reductions that could be achieved if no other constraints are taken into account, such as economy and increased demand. It can be seen as a "green scenario" that is aiming for a maximum reduction of negative externalities. In the energy sector, it is consistent with a 50% chance of limiting the average global temperature to 2 degree C (compared to pre-industrial levels). This requires that the concentrations of greenhouse gases in the atmosphere are 450 ppm of carbon dioxide equivalents. The scenario thus features the participation of major economies, such as China and India in the OECD global cap-and –trade scheme after 2020.

A ratio similar to the difference in the IPCC A1 [1] and IPCC B1 [2] scenario were applied to estimate the future consumption/production of industrial goods.

Consumption of Hg in Hg- added products are assumed to be lowered by 95% in 2035 compared to the average in 2010 and a highest possible combination of measures are being applied by all countries which includes collection and safe storage of 15% of Hg in Hg- added products, recycling of 45% of Hg in the waste stream, a lower emission factor (0.03) for controlled waste incineration, assuming at the same time that 100% of waste incineration is applied and that 80% of waste to landfills are safely controlled. Similarily use of Hg in Artisanal Gold Mining was assumed to be reduced by 46% and 76% for the NPS and 450 ppm scenarios, respectively.

2.5 Assessment of 2010 global emissions and emission factors

The recent estimate of Hg emissions to the atmosphere (targeting the year 2010) has found artisanal and small- scale gold mining as well as combustion of fossil fuels (mainly coal) for energy and heat production in power plants and in industrial and residential boilers as the major anthropogenic sources of Hg emissions to the atmosphere. These sources account for about 37% and 25% of the total Hg emissions globally, estimated to be about 2000 tonnes. Next, primary non- ferrous metals

[1] The A1 scenario describes the future world of very rapid economic growth and a rapid introduction of new and more efficient technologies. It also assumes a substantial reduction in regional differences in per capita income.

[2] The B1 scenario assumes more environmental focus a rapid change in economic structures towards a service and information economy which reduces material intensity and the introduction of clean and resource- efficient technologies. It assumes, however, no additional climate initiatives.

Atmos. Chem. Phys. Discuss., doi:10.5194/acp-2016-370, 2016
Manuscript under review for journal Atmos. Chem. Phys.
Published: 25 May 2016

Atmospheric Chemistry and Physics Discussions

production and cement production account for relatively large contributions to the emission inventory, being responsible for about 10% and 9 % respectively. Large- scale gold production and waste from consumer products (mostly landfill but also incineration) both contribute about 5% while contaminated sites are responsible for about 4%. Pig iron production contributes about 2.3% while the rest result from the chlor- alkali industry (1.4%), oil refining (0.8%), Hg production (0.6%), cremation (0.2%) as well as natural gas combustion (AMAP/UNEP, 2013).

The emissions in Asian countries, particularly in China and India dominate the total emissions of Hg. This trend has been observed from 2005 until 2010. In fact, Asian emissions also dominated the global anthropogenic emissions of mercury in the 1990s, as concluded in Pacyna et al (2010). A Hg emission trend assessment has reviled that after having peaked in the 1970`s, the total anthropogenic Hg emissions to the atmosphere appear to be relative stable between 1990 and 2005 (AMAP, 2010). A decrease in emissions in Europe and North America during the time period has been offset by an increase in Asia. The largest increase in emissions is generally due to an increase in coal burning for power and heat generation and for industrial purposes. Increased use of air pollution controls, removing mercury as a co- benefit (and some mercury specific removing technologies), have slowed down or even reduced the emissions from the increased energy demand. This is especially the case for Europe and North America, but is also reflected in new coal-fired power plants with state-of-art pollution controls installed in China (AMAP/UNEP 2013).

Spatial distribution of the global anthropogenic emissions of Hg in 2010 is presented in Fig. 2.

Fig. 2 here

The dataset on current emissions from natural sources includes contribution from primary natural sources and reemission processes of historically deposited mercury over land and sea surfaces. The most updated inventory of global natural emissions was published by Pirrone et al.,(2010). The mercury emitted from volcanoes, geothermal sources and topsoil enriched in mercury pertains to primary natural sources, whereas the re-emission of previously deposited mercury on vegetation, land or water surfaces is primarily related to land use changes, biomass burning, meteorological conditions and exchange mechanisms of gaseous mercury at air-water/top soil/snow-ice pack interfaces.

The current estimate of mercury emissions from natural processes (primary mercury emissions and re-emissions), including mercury depletion events, were estimated to be 5207 tonnes per year which represent nearly 70% of the global mercury emission budget. Oceans are the most important sources (36%) followed by biomass burning (9%), deserts, metalliferous and non-vegetated zones (7%), tundra and grassland (6%), forests (5%) and evasion after mercury depletion events (3%). Overall, the relative contribution of terrestrial surfaces is 2429 Mg per year (47%) and that from surface waters is 2778 Mg per year (53%). By considering upper and lower bounds of natural mercury emission as reported in several published papers and international reports (i.e., Sunderland and Mason 2007, Mason 2009, Pirrone et al. 2010, a Monte Carlo simulation was performed in order to evaluate the range of uncertainty for each natural emission source category.

Atmos. Chem. Phys. Discuss., doi:10.5194/acp-2016-370, 2016
Manuscript under review for journal Atmos. Chem. Phys.
Published: 25 May 2016

Atmospheric Chemistry and Physics Discussions

2.6 Assessment of global mercury emissions in the year 2035

Many variables affect future mercury emissions, however, the main ones are likely to be linked to the production and consumption of energy and industrial goods, intentional use of mercury in products, artisanal and small-scale gold mining, the use of dental amalgam, as well as increasing human population and related demands on one side, and the introduction of legislations and directives, awareness campaigns, industrial technology improvements and the increasing use of pollution control equipment on the other side.

Implementation of various climate change mitigation options to reduce carbon dioxide emissions, such as improvement of energy efficiency in power stations, replacement of fossil fuels by renewable sources, improvement of combustion, and industrial technologies, and application of carbon capture and storage (CCS) technologies are expected to have positive effects on the reduction of releases of Hg since these measures typically reduce the emissions of Hg as well as several other contaminants of concern for the environment and human health as a co- benefit. A wide range of policies are already in place (mainly in OECD countries) to encourage reduction of greenhouse gas emissions. It is expected, however, that the use of cheaper fossil fuels is likely to remain dominant in most regions to meet increasing energy demands.

Changes in energy production and consumption until the years 2035 and 2050 have been presented by the IEA WEO and Energy Technology Perspectives (ETP), respectively. In the projections, WEO focuses on certain key aspects, such as energy prices, concerns for greenhouse gas (GHG) emissions and its impacts on energy investments, the increasing use of renewable energy, changes in regulations and directives as well as recent developments in technologies for energy production. The International Panel of Climate Change (IPCC) Special Report on Emission Scenarios (SRES) (Baseline scenario A1, A2, B1 and B2) on climate change does not project any additional policies above current ones until year 2100, however they focus on socio- economic, demographic and technological change.

A comparison of the 2035 emissions estimated for various scenarios indicates that 1960, 1020 and 300 tonnes of annual mercury emissions would be emitted globally in 2035 under the CP, NP and MFR scenarios, respectively. This means that if mercury continues to be emitted under the control measures and practices that are decided at present against a background of changing population and economic growth, the 2010 emissions will remain the same in 2035. A full implementation of policy commitments and plans (the basic assumption of the NP scenario), implies a benefit of reducing mercury emissions by up to 940 tonnes per year in 2035 under the assumptions employed in this scenario. A maximum feasible emission reduction of mercury emissions results in 1 660 tonnes less emissions than those emissions envisaged under the CP scenario. The sector- and region-specific contributions to mercury emissions under the various scenarios can be observed in Figs.3 and 4.

Fig. 3 here

Fig. 4 here

Atmos. Chem. Phys. Discuss., doi:10.5194/acp-2016-370, 2016
Manuscript under review for journal Atmos. Chem. Phys.
Published: 25 May 2016

Spatial distributions of emissions within various scenarios in 2035 are presented in Figs. 5, 6, and 7 for the CP, NP and MFR scenarios, respectively.

Fig. 5 here

Fig. 6 here

Fig. 7 here

3 Model evaluation of future scenarios of mercury pollution

Various models were used to estimate current atmospheric concentrations and deposition of mercury world-wide, as well as atmospheric deposition of the contaminant in the future.

3.1 Model description

Two global chemical transport models (GLEMOS and ECHMERIT) have been used for the evaluation of future Hg pollution levels considering future emission scenarios.

GLEMOS (Global EMEP Multi-media Modelling System) is a multi-scale chemical transport model developed for the simulation of environmental dispersion and cycling of different chemicals including mercury (Travnikov and Ilyin, 2009). The model simulates atmospheric transport, chemical transformations and deposition of three Hg species (GEM, GOM and PBM). The atmospheric transport of tracers is driven by meteorological fields generated by the Weather Research and Forecast modelling system (WRF) (Skamarock et al., 2009) fed by the operational analysis data from ECMWF (ECMWF, 2016).The model has a horizontal resolution 1°×1°.Vertically, the model domain reaches 10 hPa and consists of 20 irregular terrain-following sigma layers. The atmospheric chemical scheme includes Hg redox chemical reactions in both the gaseous and aqueous phase (cloud water). Oxidized Hg species (GOM and PBM) are removed from the atmosphere by wet deposition. All three species interact with the ground contributing to dry deposition.

ECHMERIT is a global on-line chemical transport model, based on the fifth generation global circulation model ECHAM , with a highly flexible chemistry mechanism designed to facilitate the investigation of tropospheric mercury chemistry (Jung et al., 2009, De Simone et al., 2014). ECHMERIT uses T42 horizontal resolution (roughly 2.8° by 2.8° at the equator) and 19 vertical non-equidistant hybrid-sigma levels up to 10 hPa. The model simulates the physical and chemical process of three Hg species (GEM, GOM and PBM). Monthly biomass burning mercury emissions from the FINNv1 inventory are mapped

Atmos. Chem. Phys. Discuss., doi:10.5194/acp-2016-370, 2016
Manuscript under review for journal Atmos. Chem. Phys.
Published: 25 May 2016

off-line to the model (De Simone et al., 2015), whereas emissions from oceans are calculated on-line, as discussed in (De Simone et al., 2014). The so-called prompt re-emission (Selin et al., 2008) of deposited Hg is also used in the model. Hg removal processes include both dry and wet deposition of reactive species (GOM and PBM). GEM does not contribute to dry deposition. The model was run in reanalysis mode using data from the ERA-INTERIM project (ECMWF).

Both models in the base configuration consider ozone- and OH-initiated reactions as the main mechanisms of GEM oxidation in the free troposphere. It should be noted that the role and even occurrence of these reactions in the atmosphere are not certain (Goodsite et al., 2004; Hynes et al., 2009), but there is no current consensus (Subir et al., 2011; 2012). There is evidence supported by measurement data that GEM oxidation in some atmospheric environments (e.g. upper troposphere/lower stratosphere, marine boundary layer) is driven by reaction with atomic Br (Hedgecock and Pirrone, 2004; Holmes et al., 2009; Lyman and Jaffe, 2011; Obrist et al., 2011; Gratz et al., 2015). Besides, application of the Br oxidation chemistry as the only oxidation mechanism in global-scale modelling can successfully reproduce available observations of GEM concentrations and Hg wet deposition fluxes (Holmes et al., 2010; Soerensen et al., 2010; Amos et al., 2012).Nevertheless, some laboratory studies demonstrate the viability of GEM oxidation by O3 in the atmosphere in the presence of secondary organic aerosol (Rutter et al., 2012). Application of the O3 and OH chemistry as an alternative mechanism for simulation of Hg levels in the free troposphere can lead to better correlation with measurements indicating the possibility of multiple GEM oxidation pathways occurring in the atmosphere (Weiss-Penzias et al., 2015).

Therefore, taking into account the limited knowledge on the overall redox cycle of Hg in the atmosphere the well established chemical schemes based on the ozone- and OH-initiated reactions were applied in this study, which allow reasonable reproduction of the measured Hg levels on a global scale. Nevertheless, the models differ in their treatment of the forms of the oxidation products. In GLEMOS all products of GEM oxidation are treated as PBM, whereas ECHMERIT expects the products to be in the gaseous form (GOM).

Both models used the global Hg anthropogenic emission inventory for 2010 (AMAP/UNEP, 2013) for the current state and the three emission scenarios for 2035 discussed above in Section 2. However, the models use different estimates of natural and secondary emissions of Hg to the atmosphere. GLEMOS utilized prescribed monthly mean fields of Hg emission fluxes from geogenic and legacy sources (Travnikov and Ilyin, 2009), whereas ECHMERIT applied parameterisation of dynamic air-seawater exchange as a function of ambient parameters (De Simone et al., 2014). As a result, the total estimate of Hg global natural and secondary emissions by ECHMERIT (8600 t/y) is a factor of 2 higher than the total value used in GLEMOS (3995 t/y). The higher emissions in the former model are compensated by higher deposition of GEM in the air-surface exchange process. Therefore the net fluxes of Hg exchange between the atmosphere and the surface are comparable in the models.

Meteorological data for 2013 were used in all simulations to exclude the influence of inter-annual meteorological variability on the analysis results. Each model run consisted of a multi-year spin-up to reach steady-state conditions and a one-year control simulation for the analysis. It should be noted that the geogenic and legacy sources were assumed to be unchanged during the simulation period (2013-2035). Thus, the results presented reflect the response of Hg atmospheric deposition to

Atmos. Chem. Phys. Discuss., doi:10.5194/acp-2016-370, 2016
Manuscript under review for journal Atmos. Chem. Phys.
Published: 25 May 2016

changes in direct anthropogenic emissions and do not take into account the possible feedback of the ocean and terrestrial reservoirs to these changes.

3.2 Assessment of current air concentrations and atmospheric deposition of Hg

Global distributions of surface GEM concentrations simulated by two global models are shown in Fig. 8. The model results show similar spatial patterns of mercury concentrations with a pronounced gradient between the Southern and the Northern Hemispheres and elevated concentrations in major industrial regions – East and South Asia, Europe and North America., High concentrations are also seen in some regions of the tropics (the north of South America, Sub-Saharan Africa and Indonesia) due to significant Hg emissions from artisanal and small-scale gold mining. Generally, the simulated results agree satisfactorily with observations shown by circles in the figure, using the same colour palette.

Fig. 8 here

More detailed model-to-measurements comparison of GEM concentrations as well as Hg in wet deposition is shown in the scatter plots in Fig.9. As can be seen, the discrepancy between the simulated and observed concentrations of GEM does not exceed a factor of 1.5. It should be noted that the models also demonstrate acceptable performance simulating wet deposition fluxes (not shown here). However, model-to-model and model-to-observation deviations are somewhat larger in this case due to stronger effect of uncertainties in atmospheric chemistry and some meteorological parameters (e.g. precipitation amount). Thus, the models successfully reproduce the spatial patterns of Hg concentration in air and wet deposition under current conditions.

Fig. 9 here

A more challenging parameter for model simulations is the total atmospheric deposition (wet and dry). In contrast to wet deposition, the dry deposition of Hg, that describes interaction with the surface is poorly known and sparsely measured to constrain chemical transport models (Agnan et al., 2016; Zhu et al., 2016).The situation becomes even more complicated by the bi-directional character of surface uptake (Qureshi et al., 2012; Gustin, 2012). Therefore, estimates of Hg dry and, consequently, total deposition of Hg by contemporary models differ significantly (Lin et al., 2006; 2007; Bullock et al., 2008; Travnikov et al., 2010).

Figure 10 shows the global distributions of total Hg deposition flux simulated by GLEMOS and ECHMERIT for the current state. Both models estimate high deposition levels over industrial regions of East and South Asia, Europe and North America. There is also significant deposition in the tropics due to precipitation. However, there are considerable differences between the two models caused by different model formulations. ECHMERIT predicts significantly larger deposition levels

Atmos. Chem. Phys. Discuss., doi:10.5194/acp-2016-370, 2016
Manuscript under review for journal Atmos. Chem. Phys.
Published: 25 May 2016

in low and temperate latitudes, particularly, over the ocean because of intensive air-water exchange. On the other hand, GLEMOS simulates increased deposition fluxes in the polar regions due to the effect of the atmospheric mercury depletion events (Schroeder et al., 1998; Lindberg et al., 2002; Steffen et al., 2008), which are not taken into account by ECHMERIT. As shown below, the differences between the model estimates of Hg total deposition are largely caused by the contributions of natural and secondary sources (see Section 3.1).

Fig. 10 here

The majority of human exposure and health risk associated with Hg comes from consumption of marine and freshwater foods (Mahaffey et al., 2004; 2009; Sunderland et al., 2010; AMAP/UNEP, 2013). Direct atmospheric deposition is the dominant pathway of Hg entry to the ocean and freshwater environmental compartments (taking into account watersheds) (Mason et al., 2012; AMAP/UNEP, 2013). Therefore, in the following analysis the focus will be placed on changes of Hg deposition in future scenarios with respect to the current state keeping in mind significant uncertainties of available model estimates of this parameter.

3.3 Future changes of mercury deposition levels

Projections of future changes in Hg deposition on a global scale simulated by GLEMOS and EHMERIT for three emissions scenarios of 2035 are illustrated in Fig. 11. The 'Current Policy' scenario (CP 2035) predicts a considerable decrease (20-30%) of Hg deposition in Europe and North America and strong (up to 50%) increase in South and East Asia (Figs. 11a and 12b). In other parts of the Northern Hemisphere no significant changes (±5%) are expected, whereas a slight decrease (5-15%) in deposition is seen in the Southern Hemisphere.

According to the 'New Policy' scenario (NP 2035) a moderate decrease of Hg deposition (20-30%) is predicted over the whole globe except for South Asia (India), where an increase in deposition (10-15%) is expected due to the growth of regional anthropogenic emissions (Figs. 11c and 11d).

Model predictions based on the 'Maximum Feasible Reduction' scenario (MFR 2035) demonstrate consistent Hg deposition reduction on a global scale with a somewhat larger decrease in the Northern Hemisphere (35-50%) and a smaller decrease (30-35%) in the Southern Hemisphere (Figs. 11e and 11f). Thus, the most significant changes in Hg deposition (both increase and decrease) during the next 20 years for all considered scenarios are expected in the Northern Hemisphere and, in particular, in the largest industrial regions, where the majority of regulated emission sources are located.

Fig. 11 here

Atmos. Chem. Phys. Discuss., doi:10.5194/acp-2016-370, 2016
Manuscript under review for journal Atmos. Chem. Phys.
Published: 25 May 2016

Atmospheric Chemistry and Physics Discussions

4 Source apportionment of Hg deposition

Mercury is known to be a global pollutant as it is transported over long distances in the atmosphere. As has been shown in previous studies (Seigneur et al., 2004; Selin et al., 2008; Travnikov and Ilyin, 2009; Corbitt et al., 2011; Lei et al., 2013; Chen et al., 2014), atmospheric transport from distant sources can make a significant contribution to Hg deposition. Therefore, changes of Hg deposition in a region depend not only on the dynamics of local emissions but also on emission changes in other regions of the globe. The global models have been applied for source apportionment of Hg deposition for both the current state and the future scenarios. The definition of source and receptor regions adopted in the study is shown in Fig. 12. The regions considered include the continents (Europe, North, Central and South America, Africa, Australia), large sub-continents (the Middle East, countries of the Commonwealth of Independent States (CIS), South, East and Southeast Asia) and the Polar Regions.

Fig. 12 here

The dynamics of Hg deposition between 2013 and 2035 in the various geographical regions is shown in Fig. 13 along with the disintegration of the average deposition flux into direct anthropogenic and natural/legacy components. As mentioned above, both models simulate the highest Hg deposition fluxes and the most significant deposition in South, East and Southeast Asia. Mercury deposition increases or decreases by up to a factor of two in these regions depending on the scenario. All other regions are characterized by either insignificant changes (CP 2035) or moderate deposition reduction (NP 2035 and MFR 2035). The smallest changes are expected in regions remote from significant emissions sources (e.g. the Arctic and Antarctica). Deposition fluxes simulated by ECHMERIT are higher by a factor of 1.5-3 than those simulated by GLEMOS. The difference is the greatest over the oceans. It should be noted that the deviation is largely caused by differences in deposition from natural and legacy sources. Levels of Hg deposition from direct anthropogenic sources simulated by the two models are comparable. Therefore, the following source apportionment analysis was performed for the anthropogenic component of Hg deposition and presented using the mean value of the two models.

Fig. 13 here

Figure 14 shows the source apportionment of Hg deposition from direct anthropogenic sources in different geographical regions. The contribution of natural and legacy emissions is not shown in the figure. Hg deposition in South and East Asia is largely determined by domestic sources (Figs. 14a-b). In both regions the CP 2035 scenario predicts a significant increase in deposition during next 20 years. In contrast, the NP 2035 scenario forecasts increasing deposition in South Asia, but a decrease in East Asia. A strong decrease in deposition would be expected in both regions according to the MFR 2035 scenario. All three future scenarios predict a reduction of Hg deposition in North America and Europe (Figs. 14c-d). The

Atmos. Chem. Phys. Discuss., doi:10.5194/acp-2016-370, 2016
Manuscript under review for journal Atmos. Chem. Phys.
Published: 25 May 2016

decrease in Hg deposition from local sources is partly offset by an increase in deposition from Asian sources for CP 2035, whereas the other scenarios predict a reduction of Hg deposition from most anthropogenic sources. The Arctic is a remote region without significant local emission sources of Hg. Changes of Hg deposition in this region reflect the dynamics of major emission sources in the whole North Hemisphere (Fig. 14e). In spite of a significant emission reduction in Europe and North America, the Arctic is largely affected by Hg atmospheric transport from East and South Asia. As a result, no significant deposition changes are expected in this region according to CP 2035. However, the other scenarios forecast a net reduction of Hg deposition from direct anthropogenic sources in the Arctic.

Fig. 14 here

5 Concluding remarks

Monitoring the implementation of international agreements Hg emission reduction and its impacts on the environment and human health would require the improvement of various parameters, including emission inventories, model simulations of atmospheric deposition, and monitoring networks. This is particularly important for the monitoring of implementation of global and regional agreements, such as the Minamata Convention, and the EU Mercury Strategy, respectively.

Currently available global emissions inventories are quite complete and accurate for some anthropogenic sources, such as the energy and industrial sectors (an uncertainty of about 25 %). Much less accurate are the emission inventories for waste incineration and artisanal gold mining and production (perhaps up to a factor of 3 uncertainty). Major improvement of global emission inventories for anthropogenic sources is now expected as national emission inventories are now being carried out in several countries in preparation for the requirements posed by the Minamata Convention.

Future emission projections for Hg emissions from anthropogenic sources are dependent on economic development plans in individual countries, particularly energy production plans. One of the first attempts in developing such scenarios is presented in this work. Reduction of Hg in the future can be achieved as a co-benefit when reducing of emissions of greenhouse gases, as well as, through implementation of Hg-specific controls. The choice of future non-fossil energy sources will have large effects on Hg emissions: biomass combustion will continue to mobilise Hg present in the fuels (even if some of this Hg is natural) whereas non-combustion solutions such as solar or wind based power generation will of course not cause additional emissions of Hg.

Major problems still exist with the development of Hg emission inventories for natural sources and re-emission of this contaminant. Existing emission estimates vary by a factor of 3. This is difficult to accept for assessing current and future levels of atmospheric deposition of mercury. More measurements are needed to improve the accuracy of Hg releases from volcanoes, as well as from re-emission of this pollutant from contaminated sites.

Atmos. Chem. Phys. Discuss., doi:10.5194/acp-2016-370, 2016
Manuscript under review for journal Atmos. Chem. Phys.
Published: 25 May 2016

The results of this study confirm that current models can adequately simulate transport and atmospheric deposition of mercury. However, the accuracy of these simulations depend on the quality of input parameters , such as emissions data, meteorological parameters and modules describing the chemical and physical behavior of mercury and its compounds after entering the atmosphere. Taking into account the above mentioned concerns about Hg emission inventories, the models in this study could describe properly the atmospheric deposition trends at present and in the future. This has been confirmed by comparison of models estimates and ground-site measurements. It has been shown that the major environmental problem with mercury pollution is and will be in south-east Asia, where current emissions are the by far the largest, compared with emissions in other regions. Although mercury is a global pollutant, it has been shown by measurements and model estimates that the greatest air concentrations and atmospheric deposition is in the regions of the contaminant largest emissions. This is a clear message to policy makers developing plans for reduction of human and environmental exposure to mercury.

At present, reliable source – receptor techniques are available to study the relationship between emissions and atmospheric deposition of mercury on a global scale. This information is particularly important when elaborating strategies for Hg emission reductions world-wide. As in the case of dispersion models, the quality of estimates using the source – receptor techniques depends on many factors, including the quality of emission data, and the accuracy of measurements and model simulation of Hg atmospheric deposition. This important issue has been discussed recently in Pirrone et al. (2013) and Gustin et al. (2016).

The EU GMOS project has proved to be a very important research instrument for supporting, first the scientific justification for the Minamata Convention, and then monitoring of the implementation of targets of this Convention, as well as, the EU Mercury Strategy. This project provided the state-of-the art with regard to the development of the latest emission inventories for mercury, future emission scenarios, dispersion modelling of atmospheric Hg on global and regional scale, and source – receptor techniques for Hg emission apportionment on a global scale. It should be added that the GMOS project developed a most comprehensive monitoring network to measure mercury in the air and water (www.gmos.eu). However, the monitoring part of GMOS was largely beyond the scope of this paper. The GMOS project should be regarded as a first step in development of the Minamata Convention structure for tracing the implementation of its targets and development of future scenarios of Hg contamination of the environment. The GMOS project can be regarded as pioneering work in the important issues of tracing the effectiveness of the Minamata Convention implementation tools. The results of the GMOS project highlight the need to further improve information on emissions, state, impacts and policy response to Hg pollution on a global scale.

Acknowledgements

The results of the EU GMOS project have been obtained with financial support from the EC (Grant Agreement No. 265113). The authors are grateful for this support.

Atmos. Chem. Phys. Discuss., doi:10.5194/acp-2016-370, 2016
Manuscript under review for journal Atmos. Chem. Phys.
Published: 25 May 2016

The authors would also like to thank other scientists from the GMOS project for the possibility of using the measurement data when discussing the outcome of model simulations with monitored data.

References

Agnan Y., Le Dantec T., Moore C.W., Edwards G.C., Obrist D. (2016) New Constraints on Terrestrial Surface–Atmosphere Fluxes of Gaseous Elemental Mercury Using a Global Database. Environ. Sci. Technol. 50 (2), 507–524

AMAP, (2010). Updating Historical Global Inventories of Anthropogenic Mercury Emissions to Air. AMAP Technical Report No. 3 (2010), Arctic Monitoring and Assessment Programme (AMAP), Oslo, Norway.

AMAP/UNEP (2013) Technical Background Report for the Global Mercury Assessment 2013. Arctic Monitoring and Assessment Programme, Oslo, Norway / UNEP Chemicals Branch, Geneva, Switzerland. vi + 263 pp. (http://www.amap.no/documents/download/1265)

Ambio (2007) Special issue. Swain E.B., Jakus P.M., Rice G., Lupi F., Maxson P.A., Pacyna J.M., Penn A.F., Spiegel S.J. and M.M. Veiga. Socioeconomic consequences of mercury use and pollution. Ambio, 36,1, 45-61.

Amos H.M., Jacob D.J., Holmes C.D., Fisher J.A., Wang Q., Yantosca R.M., Corbitt E.S., Galarneau E., Rutter A.P., Gustin M.S., Steffen A., Schauer J.J., Graydon J.A., Louis V.L. St., Talbot R.W., Edgerton E.S., Zhang Y., Sunderland E.M. (2012) Gas-particle partitioning of atmospheric Hg(II) and its effect on global mercury deposition. Atmos. Chem. Phys. 12, 591–603

Bullock O.R., Atkinson D., Braverman T., Civerolo K., Dastoor A., Davignon D., Ku J.-Y., Lohman K., Myers T.C., Park R.J., Seigneur C., Selin N.E., Sistla G., Vijayaraghavan K. (2008) The North American Mercury Model Intercomparison Study (NAMMIS): Study description and model-to-model comparisons. Journal of Geophysical Research 113, D17310

Chen L., Wang H.H., Liu J.F., Tong Y.D., Ou L.B., Zhang W., Hu D., Chen C., and Wang X.J. (2014) Intercontinental transport and deposition patterns of atmospheric mercury from anthropogenic emissions. Atmos. Chem. Phys., 14, 10163–10176

Corbitt E.S, D.J. Jacob, C.D. Holmes, D.G. Streets and E.M. Sunderland (2011) Global source-receptor relationships for mercury deposition under present-day and 2050 emissions scenarios. Environmental Science and Technology, 45:10477-10484

De Simone F., Gencarelli C., Hedgecock I., Pirrone N. (2014) Global atmospheric cycle of mercury: a model study on the impact of oxidation mechanisms. Environmental Science and Pollution Research 21 (6), 4110-4123

De Simone F., Cinnirella S., Gencarelli C.N., Yang X., Hedgecock I.M., Pirrone N. (2015) Model Study of Global Mercury Deposition from Biomass Burning. Environ. Sci. Technol. 49 (11), 6712–6721

Goodsite M., Plane J., Skov H. (2004) A theoretical study of the oxidation of Hg0 to HgBr2 in the troposphere, Environ. Sci. Technol. 38, 1772–1776

Gratz L.E., Ambrose J.L., Jaffe D.A., Shah V., Jaeglé L., Stutz J., Festa J., Spolaor M., Tsai C., Selin N.E., Song S., Zhou X., Weinheimer A.J., Knapp D.J., Montzka D.D., Flocke F.M., Campos T.L., Apel E., Hornbrook R., Blake N.J., Hall S., Tyndall G.S., Reeves M., Stechman D., Stell M. (2015) Oxidation of mercury by bromine in the subtropical Pacific free troposphere. Geophys. Res. Lett. 42(23) 10,494–10,502.

Gustin M. (2012) Exchange of mercury between the atmosphere and terrestrial ecosystems, in Environmental Chemistry and Toxicology of Mercury (eds G. Liu, Y. Cai and N. O'Driscoll), John Wiley & Sons, Inc., Hoboken, NJ, USA. doi: 10.1002/9781118146644.ch10

Gustin M.S., Evers D.C., Bank M.S., Hammerschmidt C.R., Pierce A., Basu N., Blum J., Bustamante P., Chen C., Driscoll C.T., Horvat M., Jaffe D., Pacyna J.M., Pirrone N. and N. Selin.(2016) Importance of integration and implementation of emerging and future mercury research into the Minamata Convention, Environmental Science and Technology, (DOI: 10.1021/acs.est.6b00573)

ECMWF (2016) European Centre for Medium-Range Weather Forecasts http://www.ecmwf.int/en/forecasts/datasets. Accessed 20 Jan 2016.

Hedgecock I.M., Pirrone N. (2004) Chasing quicksilver: Modeling the atmospheric lifetime of Hg-(g)(0) in the marine boundary layer at various latitudes. Environmental Science and Technology, 38:69-76

Holmes, C.D., Jacob D.J., Mason R.P., Jaffe D.A. (2009) Sources and deposition of reactive gaseous mercury in the marine atmosphere. Atmospheric Environment 43(14), 2278-2285

Holmes C.D., Jacob D.J., Corbitt E.S., Mao J., Yang X., Talbot R., Slemr F. (2010) Global atmospheric model for mercury including oxidation by bromine atoms. Atmos. Chem. Phys. 10, 12037–12057

Hynes, A. J., Donohoue, D. L., Goodsite, M. E., and Hedgecock, I. M. (2009) Our current understanding of major chemical and physical processes affecting mercury dynamics in the atmosphere and at the air-water/terrestrial interfaces, in: Mercury Fate and Transport in the Global Atmosphere, edited by: Mason, R. and Pirrone, N., Springer, New York, 427–457

Jung G., Hedgecock I.M., Pirrone N. (2009) ECHMERIT V1.0 – a new global fully coupled mercury-chemistry and transport model. Geosci. Model Dev. 2, 175-195

Lei H., Liang X.-Z., Wuebbles D. J., and Tao Z. (2013) Model analyses of atmospheric mercury: present air quality and effects of transpacific transport on the United States. Atmos. Chem. Phys., 13, 10807–10825

Lin C.-J., Pongprueksa P., Lindberg S.E., Pehkonen S.O., Byun D. and Jang C. (2006) Scientific uncertainties in atmospheric mercury models I: Model science evaluation. Atmospheric Environment 40, 2911-2928.

Lin C.-J., Pongprueksa P., Lindberg S.E., Pehkonen S.O., Jang C., Braverman T. and Ho T.C. (2007) Scientific uncertainties in atmospheric mercury models II: Sensitivity analysis in the CONUS domain. Atmospheric Environment 41, 6544-6560.

Lindberg S.E., Brooks S., Lin C.-J., Scott K.J., Landis M.S., Stevens R.K., Goodsite M., and Richter A. (2002) Dynamic oxidation of gaseous mercury in the Arctic troposphere at polar sunrise. Environ. Sci. Technol. 36, 1245–1256

Lyman, S. N. and Jaffe, D. A. (2011) Formation and fate of oxidized mercury in the upper troposphere and lower stratosphere, Nat. Geosci., 5, 114–117

Mahaffey, K. R., et al. (2004), Blood organic mercury and dietary mercury intake: National Health and Nutrition Examination Survey, 1999 and 2000, Environmental Health Perspectives, 112(5): 562-670.

Mahaffey, K., et al. (2009), Adult women's blood mercury concentrations vary regionally in USA: Association with patterns of fish consumption (NHANES 1999-2004), Environmental Health Perspectives, 117(1): 47-53.

Mason, R. (2009). Mercury emissions from natural sources and their importance in the global mercury cycle. In Mercury Fate and Transport in the Global Atmosphere; Pirrone, N., Mason, R., Eds.;Springer Science+Business Media: Berlin/Heidelberg, Germany

Mason R.P., Choi A.L., Fitzgerald W.F., Hammerschmidt C.R., Lamborg C.H., Soerensen A.L. and Sunderland E.M. (2012) Mercury biogeochemical cycling in the ocean and policy implications. Environmental Research 119, 101-117

Obrist, D., Tas E., Peleg M., Matveev V., Faïn X., Asaf D., Luria M. (2011) Bromine-induced oxidation of mercury in the mid-latitude atmosphere. Nature Geoscience 4, 22-26

Qureshi A., Macleod M., Sunderland E., Hungerbühler K. (2012) Exchange of elemental mercury between the oceans and the atmosphere, in Environmental Chemistry and Toxicology of Mercury (eds G. Liu, Y. Cai and N. O'Driscoll), John Wiley & Sons, Inc., Hoboken, NJ, USA. doi: 10.1002/9781118146644.ch10

Pacyna, E.G., Pacyna, J.M., Sundseth, K., Munthe, J., Kindbom, K., Wilson, S., Steenhuisen, F., and Maxson, P. (2010). Global emission of mercury to the atmosphere from anthropogenic sources in 2005 and projections to 2020. Atmospheric Environment 44 2487-2499.

Pirrone, N., Cinnirella, S., Feng, X., Finkelman, R.B, Friedli, H.R., Leaner, J., Mason, R., Mukherjee, A.B. and Stracher, G.B., and D.G. Streets (2010). Global mercury emissions to the atmosphere from anthropogenic and natural sources. Atmos. Chem. Phys. 10, 5951–5964.

Pirrone N., Aas W., Cinnirella S., Ebinghaus R., Hedgecock I.M., Pacyna J.M., Sprovieri F. And E.M. Sunderland.(2013). Toward to next generation of air quality monitoring: Mercury. Atmospheric Environment, 80, 599-611.

Rutter A.P., Shakya K.M., Lehr R., Schauer J.J., Griffin R.J. (2012) Oxidation of gaseous elemental mercury in the presence of secondary organic aerosols. Atmospheric Environment 59, 86-92

Seigneur C, Vijayaraghavan K, Lohman K, Karamchandani P, Scott C. (2004) Global source attribution for mercury deposition in the United States. Environmental Science and Technology 38, 555-569

Selin N.E., Jacob D.J., Yantosca R.M., Strode S., Jaegle L., Sunderland E.M. (2008) Global 3-D land-ocean-atmosphere model for mercury: Present-day versus preindustrial cycles and anthropogenic enrichment factors for deposition. Global Biogeochem. Cycles 22, GB2011

Skamarock, W. C., J. B. Klemp, J. Dudhia, D. O. Gill, D. M. Barker, W. Wang, J. G. Powers, 2007: A description of the Advanced Research WRF Version 2. NCAR/TN-468+STR.. NCAR Technical Note. Boulder, CO, USA.Travnikov, O., and

Ilyin I. (2009) The EMEP/MSC-E mercury modelling system, in mercury fate and transport in the global atmosphere, edited by N. Pirrone and R. P. Mason, pp. 571-587, Springer, Dordecht

Schroeder W.H., Anlauf K.G., Barrie L.A., Lu J.Y., Steffen A., Schneeberger D.R., and Berg T. (1998) Arctic springtime depletion of mercury. Nature 394, 331–332.

Soerensen A.L., Skov H., Jacob D.J., Soerensen B.T., Johnson M.S. (2010) Global concentrations of gaseous elemental mercury and reactive gaseous mercury in the marine boundary layer. Environ. Sci. Technol. 44, 425–427

Steffen A., Douglas T., Amyot M., Ariya P., Aspmo K., Berg T., Bottenheim J., Brooks S., Cobbett F., Dastoor A., Dommergue A., Ebinghaus R., Ferrari C., Gardfeldt K., Goodsite M. E., Lean D., Poulain A. J., Scherz C., Skov H., Sommar J., and Temme C. (2008) A synthesis of atmospheric mercury depletion event chemistry in the atmosphere and snow. Atmos. Chem. Phys. 8, 1445–1482

Subir M., Ariya P.A. and Dastoor A.P. (2011) A review of uncertainties in atmospheric modeling of mercury chemistry I. Uncertainties in existing kinetic parameters – Fundamental limitations and the importance of heterogeneous chemistry. Atmospheric Environment 45, 5664-5676.

Subir M., Ariya P.A. and Dastoor A.P. (2012) A review of the sources of uncertainties in atmospheric mercury modeling II. Mercury surface and heterogeneous chemistry – A missing link. Atmospheric Environment 46, 1-10

Sunderland, E.M. and R.P. Mason, (2007) Human impacts on open ocean mercury concentrations. Glob. Biogeochem. Cycles, 21, doi:10.1029/2006GB002876.

Sunderland E., Corbitt E., Cossa D., Evers D., Friedli H., Krabbenhoft D., Levin L., Pirrone N., Rice G. (2010) Impacts of Intercontinental Mercury Transport on Human & Ecological Health. In: Pirrone, N. and T. Keating, 2010. Hemispheric Transport of Air Pollution 2010. Part B: Mercury, pp. 97-144. Air Pollution Studies No. 16. United Nations.

Sundseth K., Pacyna J.M., Pacyna E.G., Munthe J., Belhej M. and S. Astrom. (2010)Societal costs of continuing the status-quo of mercury pollution. Journal Of Cleaner Production, 18, 386 – 394, also selected for inclusion in Science for Environment Policy, the European Commission's environmental news service for policy makers, distributed to over 11,000 subscribers.

Sundseth, K. (2012) A novel combination of methods developed for decision support on abatement of mercury in Europe. Doctoral Thesis, Gdansk University of Technology (GUT), Chemical Department, Gdansk, Poland, 2012.

Sundseth K., Pacyna J.M., Banel A., Pacyna E.G. and A. Rautio.(2015) Climate change impacts on environmental and human exposure to mercury in the Arctic. Int.J.Environ.Res. Public Health, 12, 3579 – 3599 (doi:10.3390/ijerph120403579).

Travnikov O., Ilyin I. (2009) The EMEP/MSC-E Mercury Modeling System, in Mercury Fate and Transport in the Global Atmosphere: Emissions, Measurements, and Models, edited by N. Pirrone and R. P. Mason, Springer, pp. 571-587

Travnikov O., Lin C.J., Dastoor A., Bullock O.R., Hedgecock I., Holmes C., Ilyin I., Jaegle L., Jung G., Pan L., Pongprueksa P., Ryzhkov A., Seigneur C., and Skov H. (2010) Global and Regional Modeling, in: Hemispheric Transport of Air Pollution. Part B: Mercury, edited by: Pirrone, N. and Keating, T., United Nations, 97–144

UNEP (2013) The Minamata Convention on Mercury. Available at http://www.mercuryconvention.org/Portals/11/documents/Booklets/Minamata%20Convention%20on%20Mercury_booklet_English.pdf

Weiss-Penzias P., Amos H.M., Selin N.E., Gustin M.S., Jaffe D.A., Obrist D., Sheu G.-R., Giang A. (2015) Use of a global model to understand speciated atmospheric mercury observations at five high-elevation sites. Atmos. Chem. Phys., 15, 1161–1173

WEO, 2012. World Energy Outlook 2012. International Energy Agency (IEA). Paris, France.

Zhu W., Lin C.-J., Wang X., Sommar J., Fu X.W., Feng X. (2016) Global Observations and Modeling of Atmosphere-Surface Exchange of Elemental Mercury – A Critical Review, Atmos. Chem. Phys. Discuss., doi:10.5194/acp-2015-1064

Atmos. Chem. Phys. Discuss., doi:10.5194/acp-2016-370, 2016
Manuscript under review for journal Atmos. Chem. Phys.
Published: 25 May 2016

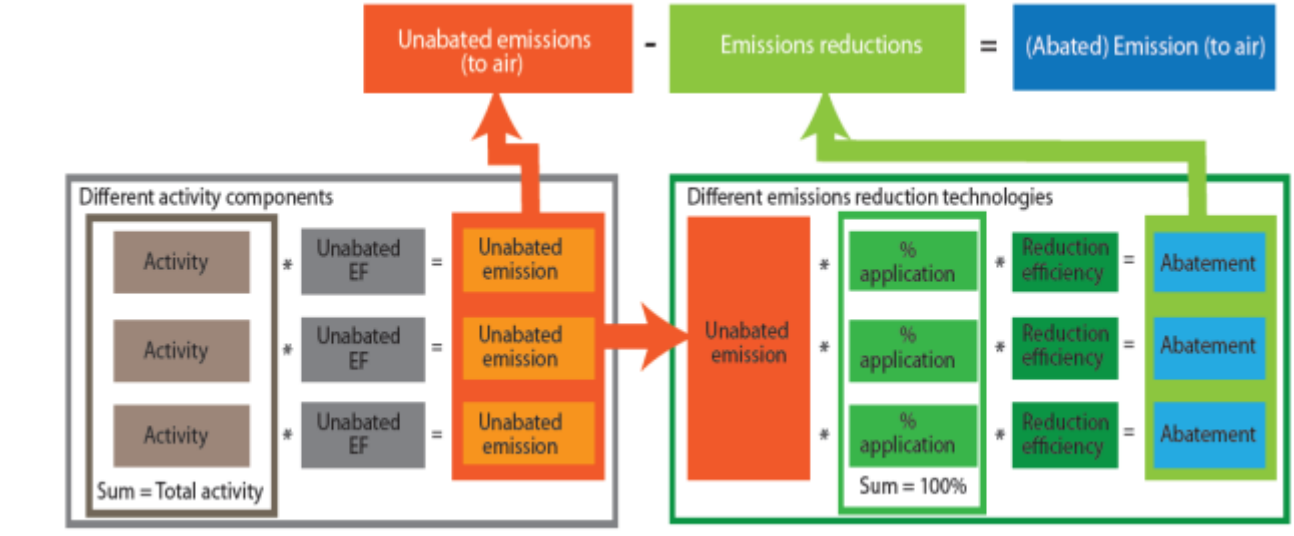

Figure 1: Methodology for 2010 emission inventory (from AMAP/UNEP, 2013).

Atmos. Chem. Phys. Discuss., doi:10.5194/acp-2016-370, 2016
Manuscript under review for journal Atmos. Chem. Phys.
Published: 25 May 2016

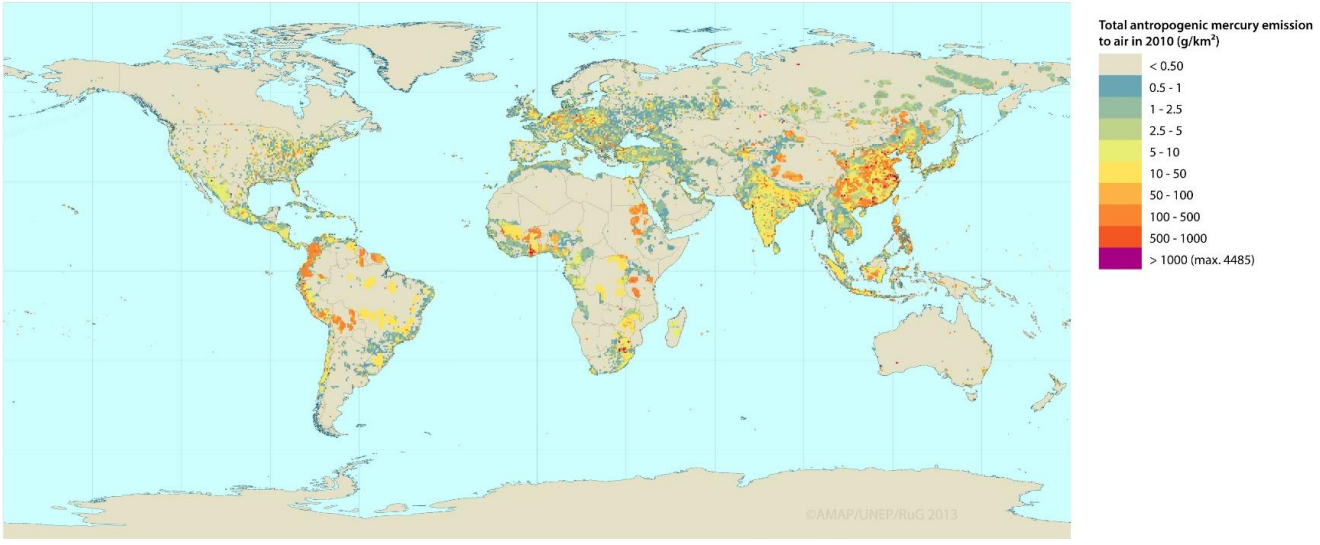

Figure 2: Spatial distribution of global anthropogenic emissions of mercury in 2010.

Atmos. Chem. Phys. Discuss., doi:10.5194/acp-2016-370, 2016
Manuscript under review for journal Atmos. Chem. Phys.
Published: 25 May 2016

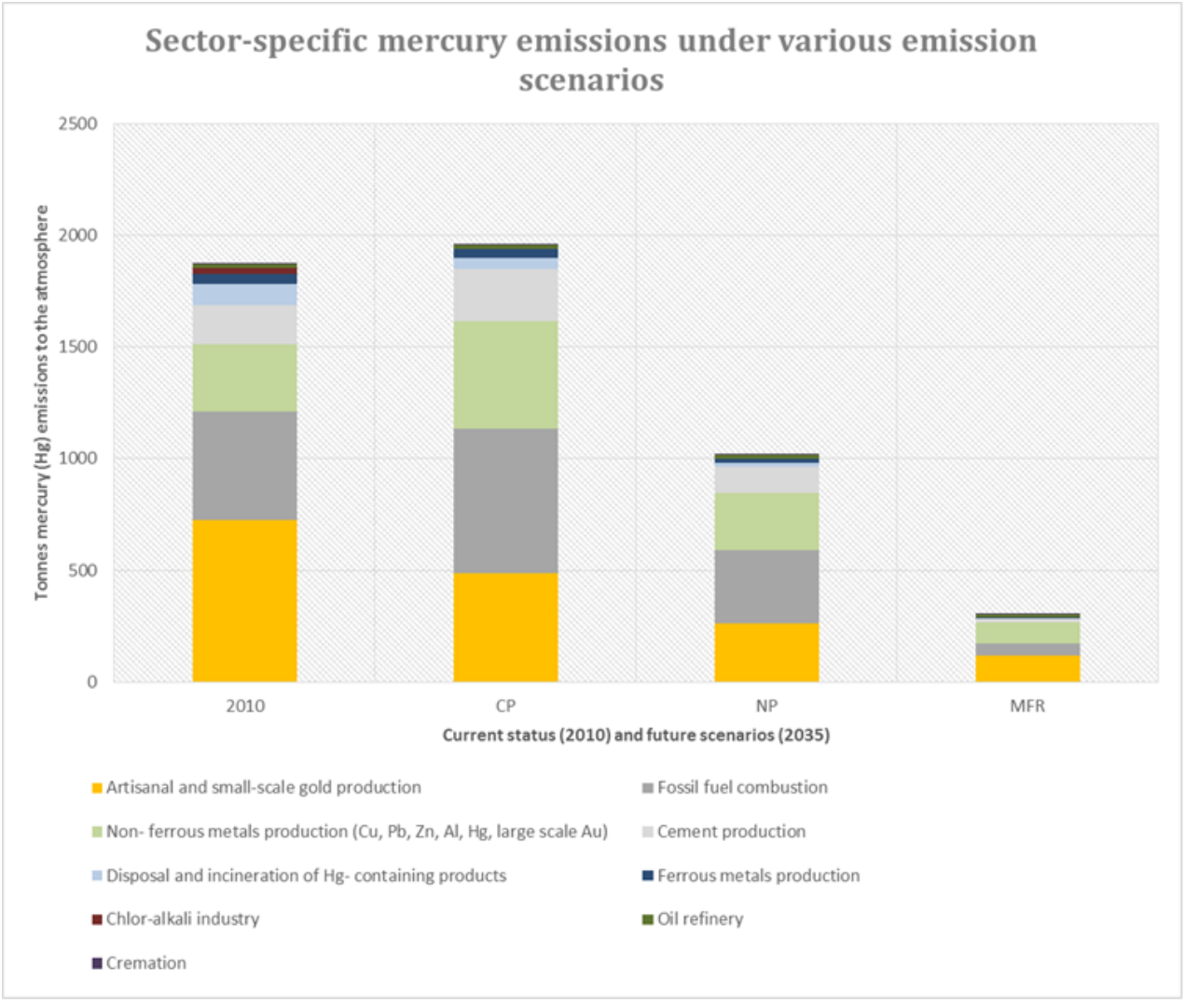

Fig. 3. Sector specific emissions of Hg under various emission scenarios in 2035.

Atmos. Chem. Phys. Discuss., doi:10.5194/acp-2016-370, 2016
Manuscript under review for journal Atmos. Chem. Phys.
Published: 25 May 2016

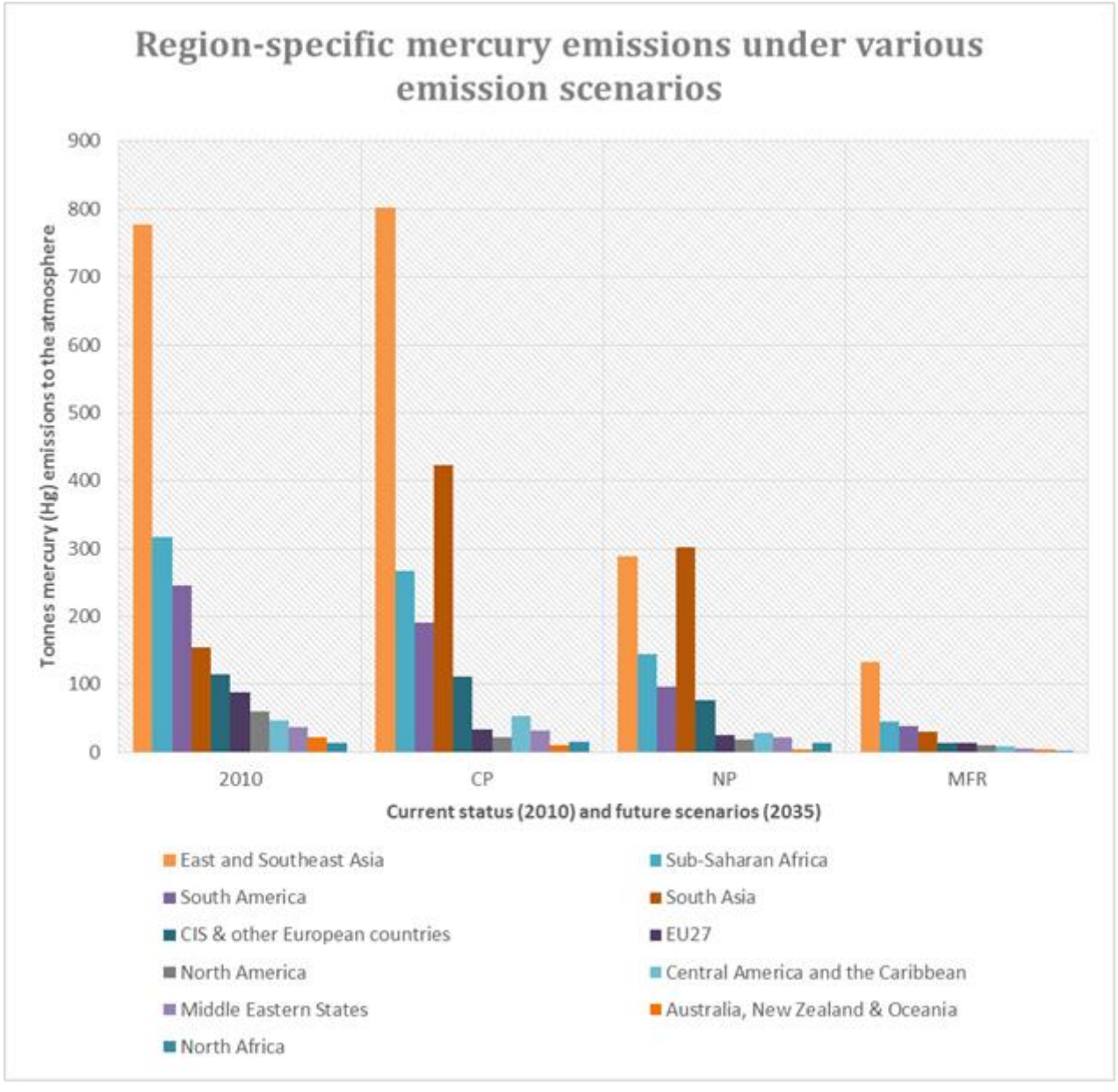

Fig. 4. Region specific emissions of Hg under various emission scenarios in 2035.

Atmos. Chem. Phys. Discuss., doi:10.5194/acp-2016-370, 2016
Manuscript under review for journal Atmos. Chem. Phys.
Published: 25 May 2016

Atmospheric Chemistry and Physics Discussions

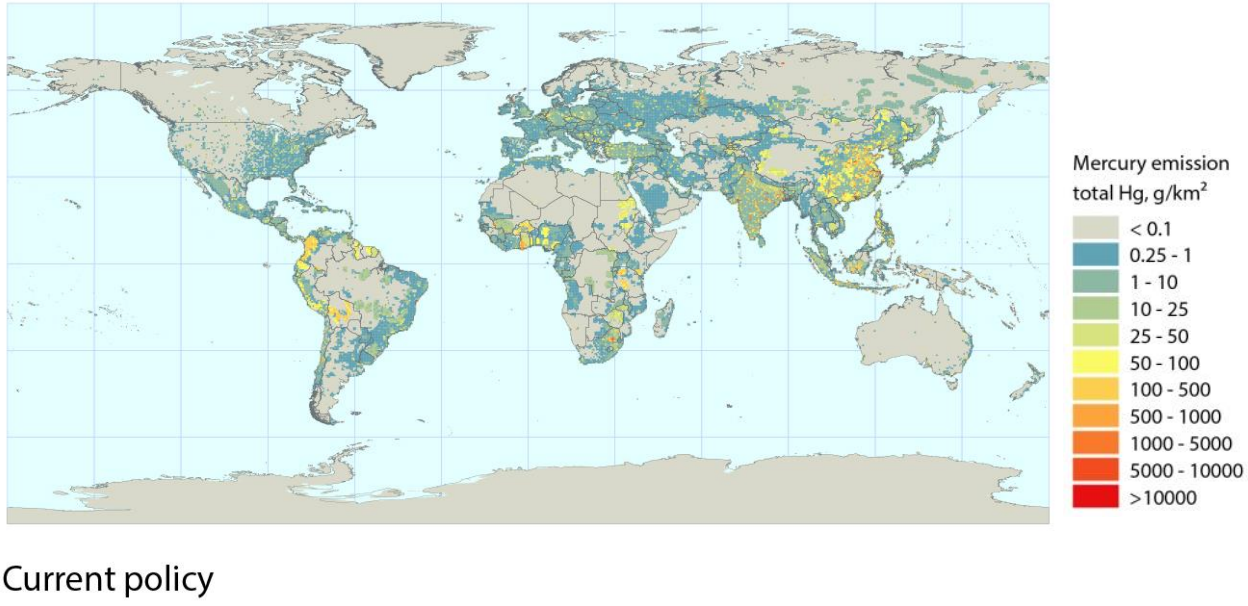

Fig. 5. Spatial distribution of Hg emissions in 2035 according to the CP scenario.

5

Atmos. Chem. Phys. Discuss., doi:10.5194/acp-2016-370, 2016
Manuscript under review for journal Atmos. Chem. Phys.
Published: 25 May 2016

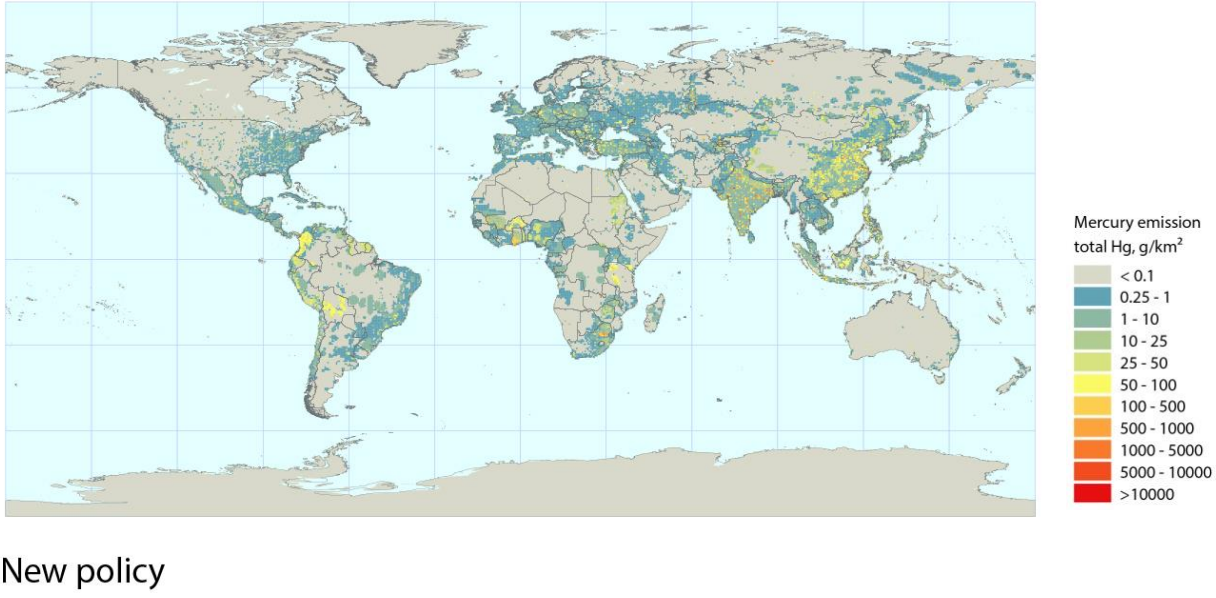

Fig. 6. Spatial distribution of Hg emissions in 2035 according the the NP scenario.

Atmos. Chem. Phys. Discuss., doi:10.5194/acp-2016-370, 2016
Manuscript under review for journal Atmos. Chem. Phys.
Published: 25 May 2016

Atmospheric Chemistry and Physics Discussions

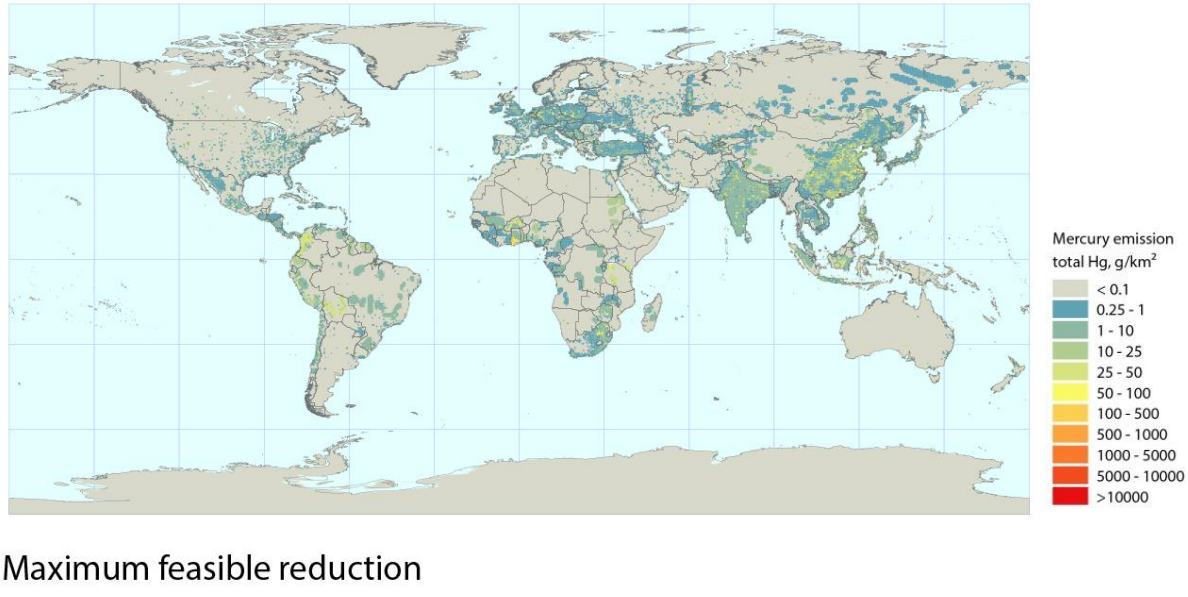

Fig. 7. Spatial distribution of Hg emissions in 2035 according the the MFR scenario.

Atmos. Chem. Phys. Discuss., doi:10.5194/acp-2016-370, 2016
Manuscript under review for journal Atmos. Chem. Phys.
Published: 25 May 2016

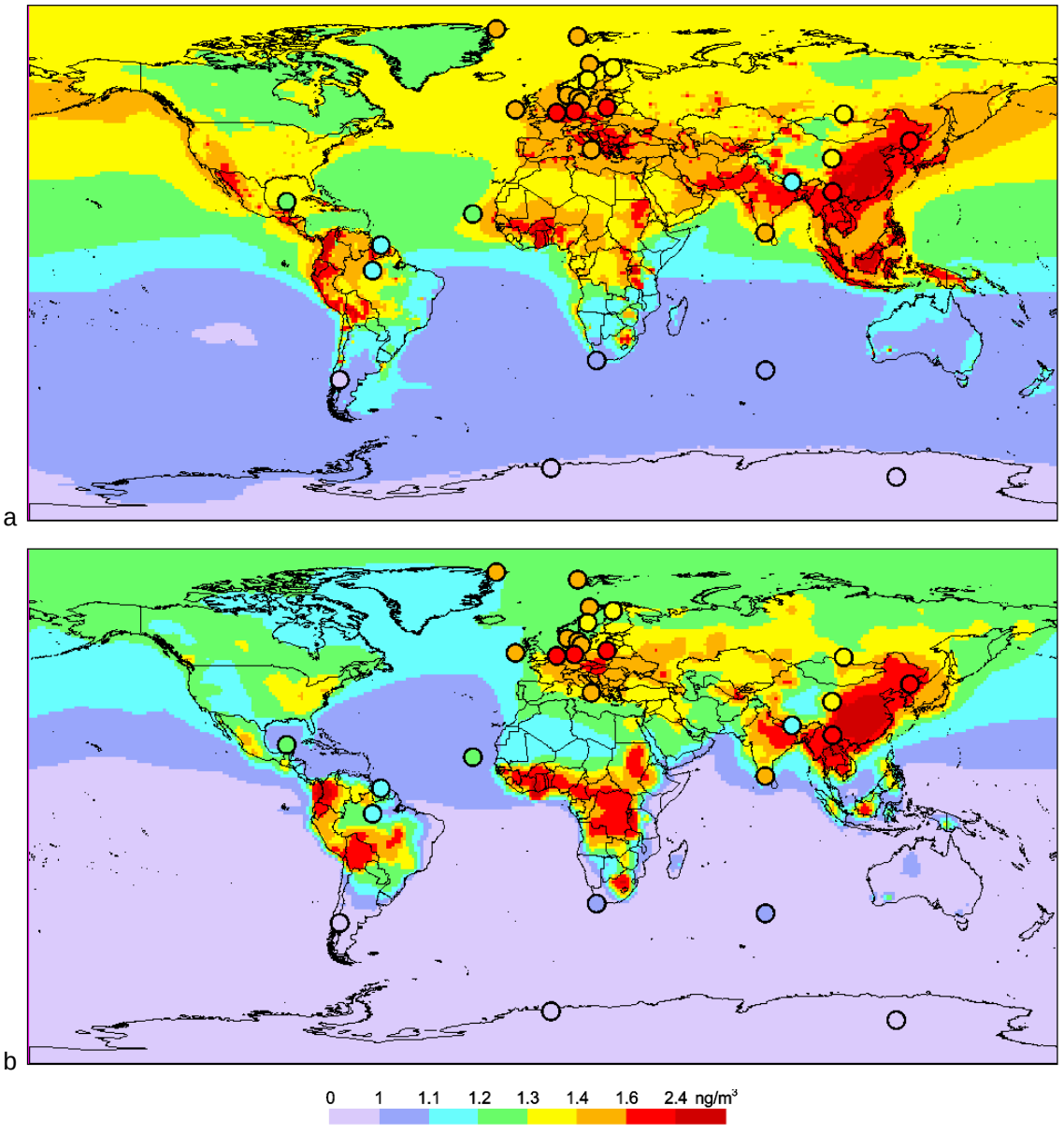

Fig. 8. Global distribution of annual mean GEM concentration in near-surface air in 2013 simulated by GLEMOS (a) and ECHMERIT (b). Circles present observed values at GMOS and EMEP ground-based monitoring sites (Annex A, Table A.1).

Atmos. Chem. Phys. Discuss., doi:10.5194/acp-2016-370, 2016
Manuscript under review for journal Atmos. Chem. Phys.
Published: 25 May 2016

Atmospheric Chemistry and Physics Discussions

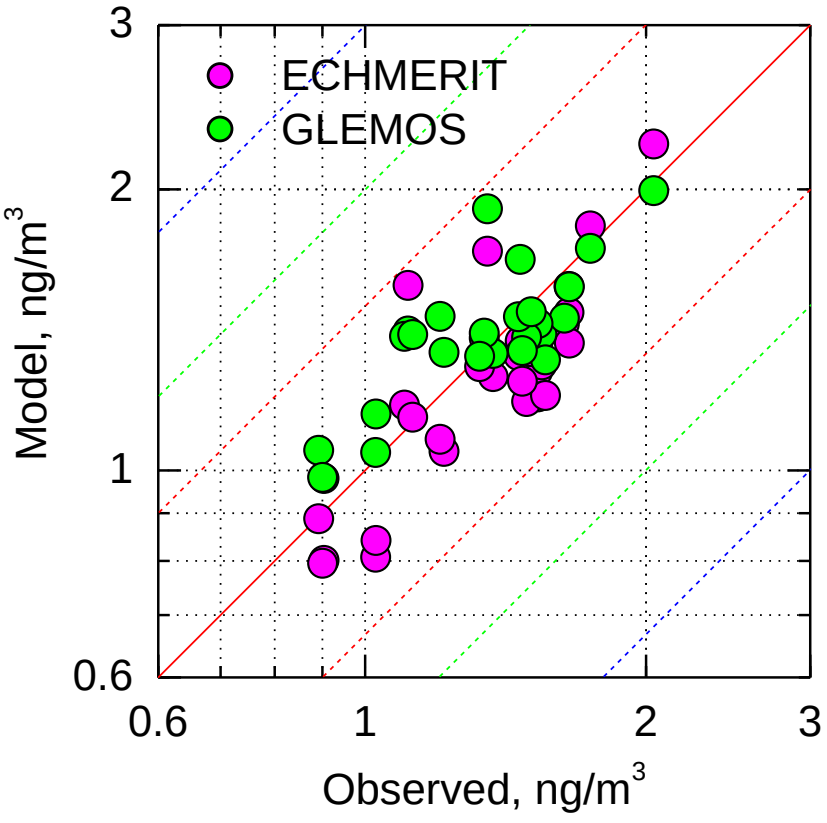

Fig. 9. Scatter-plots of annual mean GEM air concentration in 2013 measured at GMOS and EMEP ground-based sites (Annex A, Table A.1) vs. simulated by GLEMOS and ECHMERIT. Red solid line depicts the 1:1 ratio; dashed lines show different deviation levels: red – by factor of 1.5, green – by factor of 2, blue – by factor of 3.

5

Atmos. Chem. Phys. Discuss., doi:10.5194/acp-2016-370, 2016
Manuscript under review for journal Atmos. Chem. Phys.
Published: 25 May 2016

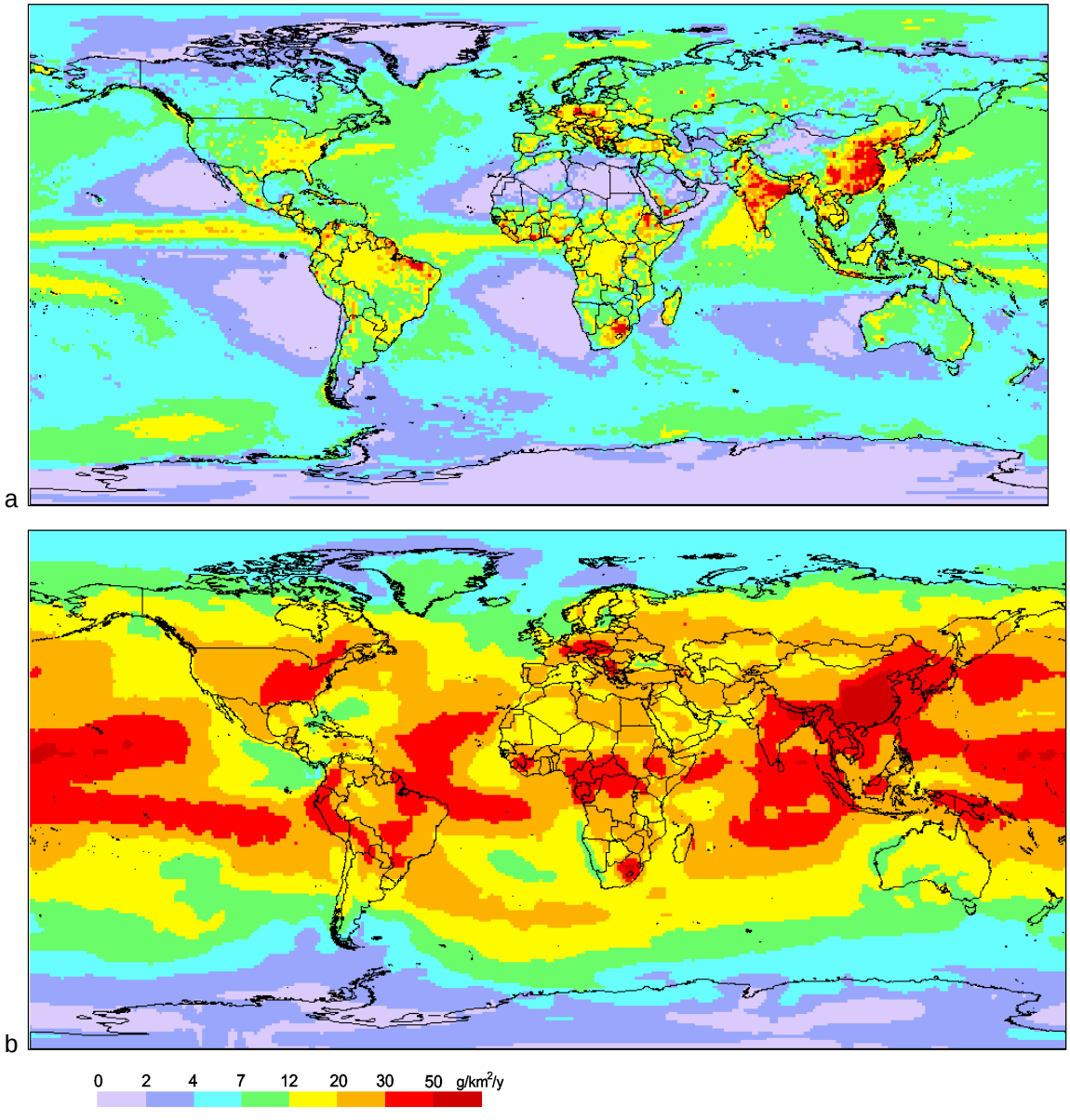

Fig. 10. Global distribution of total (wet+dry) Hg deposition flux in 2013 simulated by GLEMOS (a) and ECHMERIT (b).

Atmos. Chem. Phys. Discuss., doi:10.5194/acp-2016-370, 2016
Manuscript under review for journal Atmos. Chem. Phys.
Published: 25 May 2016

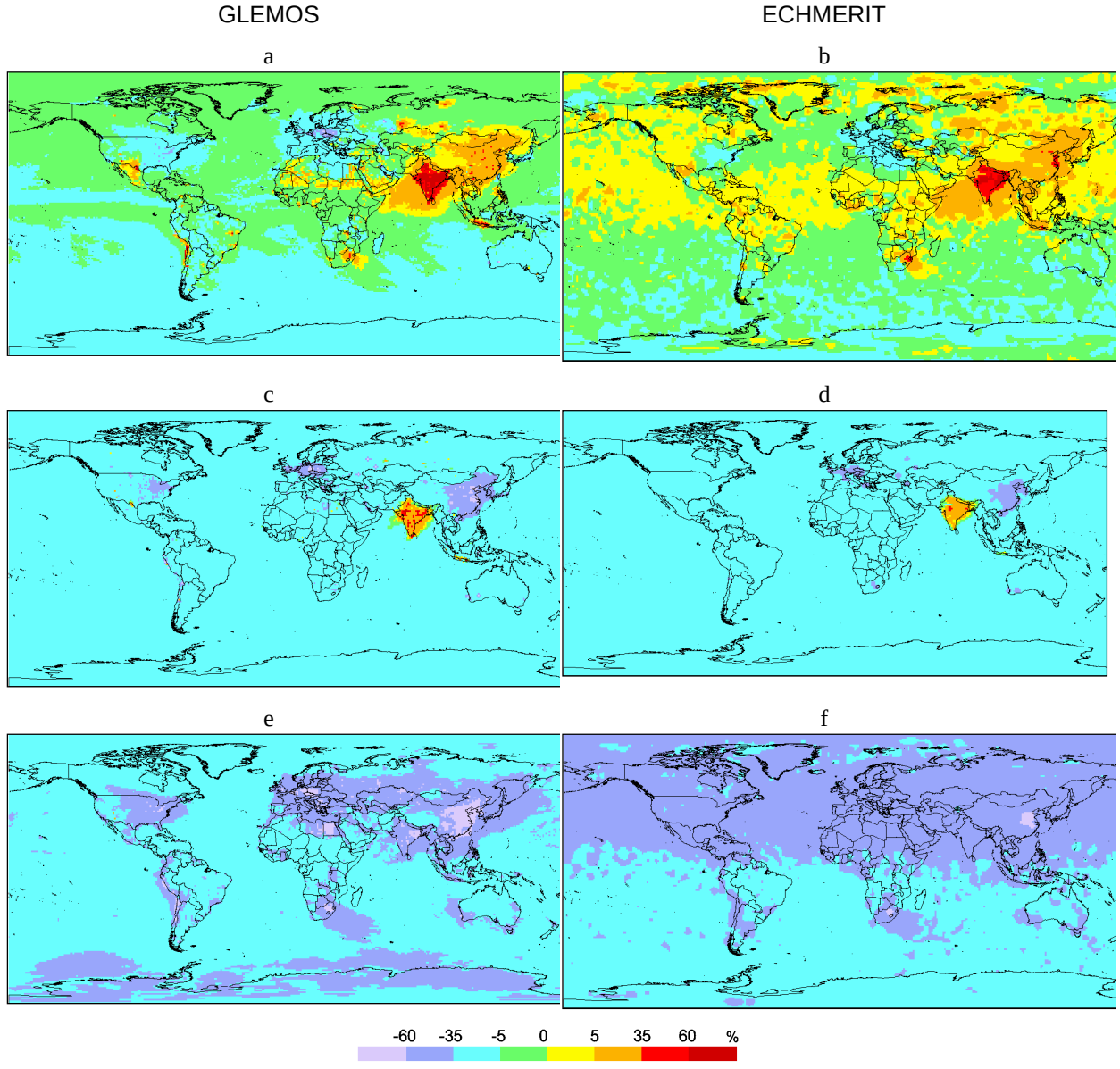

Fig. 11. Global distribution of relative changes of Hg deposition flux between 2010 and 2035 with respect to 3 emission scenarios: (a, b) – CP2035; (c, d) – NP2035; (e, f) – MFR2035. Results of GLEMOS and ECHMERIT simulations are presented in the left and right columns, respectively.

Atmos. Chem. Phys. Discuss., doi:10.5194/acp-2016-370, 2016
Manuscript under review for journal Atmos. Chem. Phys.
Published: 25 May 2016

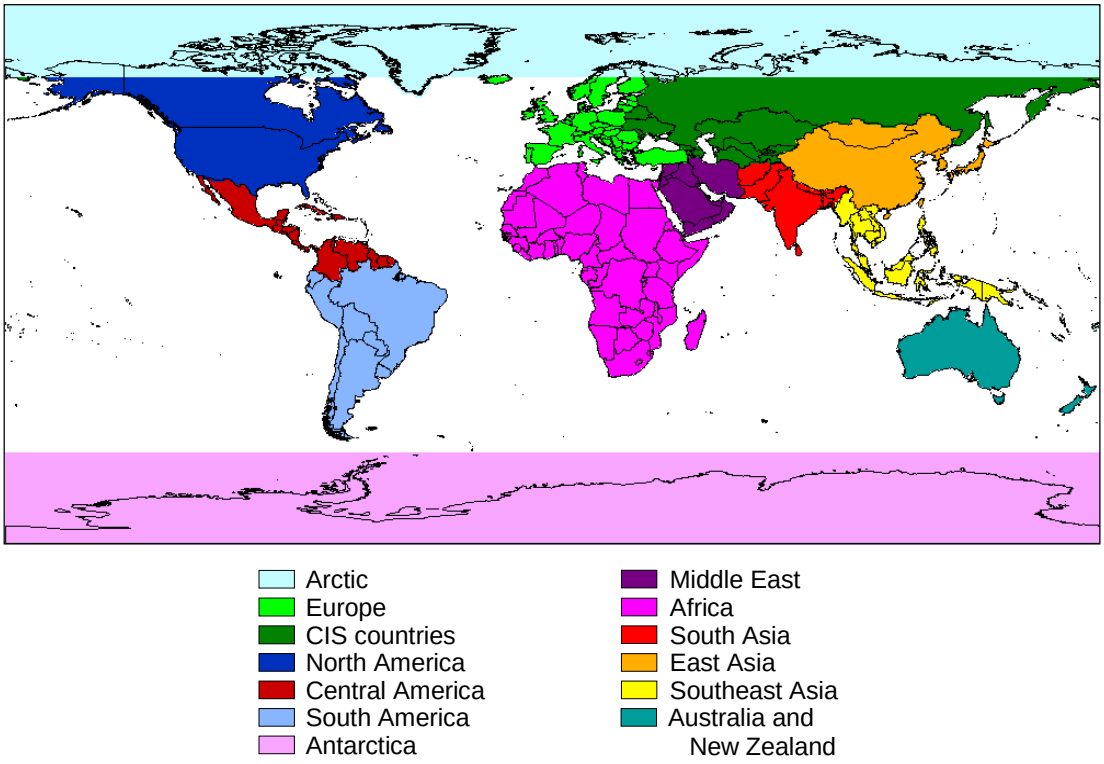

Fig. 12. Definition of source and receptor regions used in the analysis.

Atmos. Chem. Phys. Discuss., doi:10.5194/acp-2016-370, 2016
Manuscript under review for journal Atmos. Chem. Phys.
Published: 25 May 2016

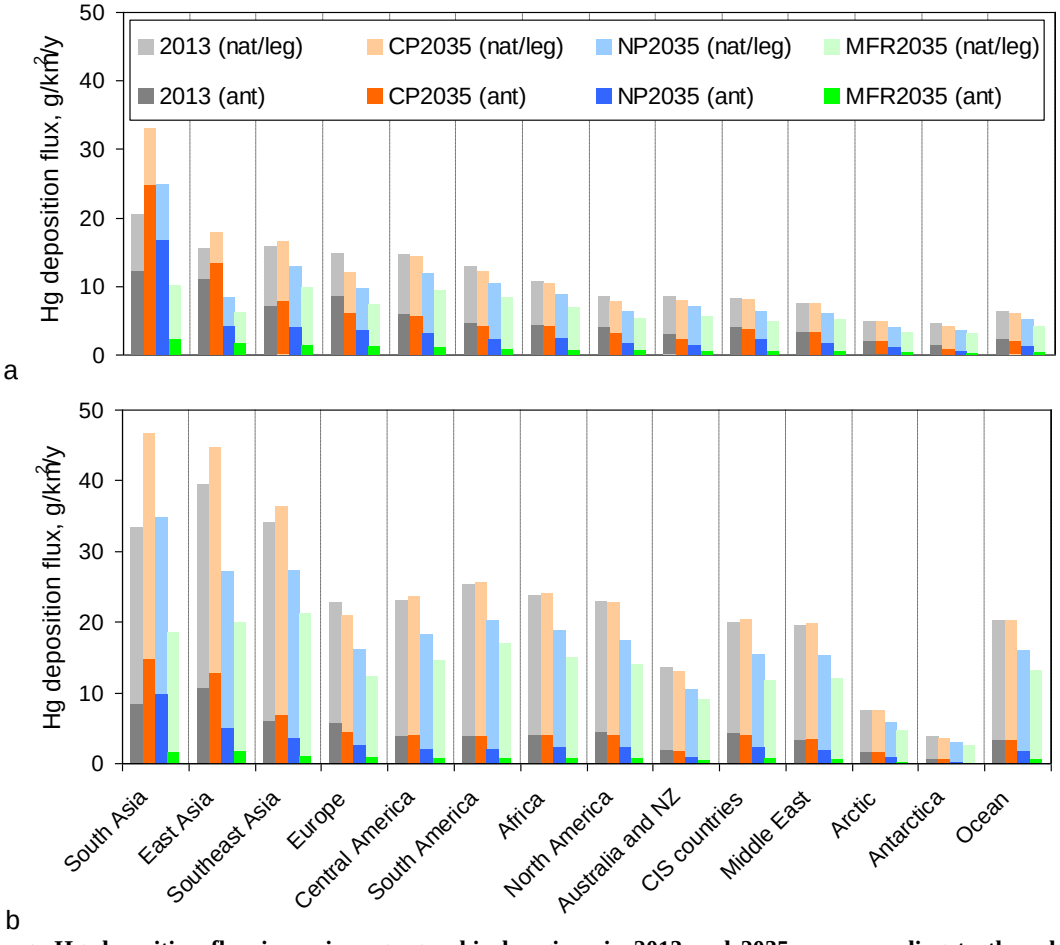

Fig. 13. Average Hg deposition flux in various geographical regions in 2013 and 2035 corresponding to the selected emission scenarios as simulated by GLEMOS (a) and ECHMERIT (b).

Atmos. Chem. Phys. Discuss., doi:10.5194/acp-2016-370, 2016
Manuscript under review for journal Atmos. Chem. Phys.
Published: 25 May 2016

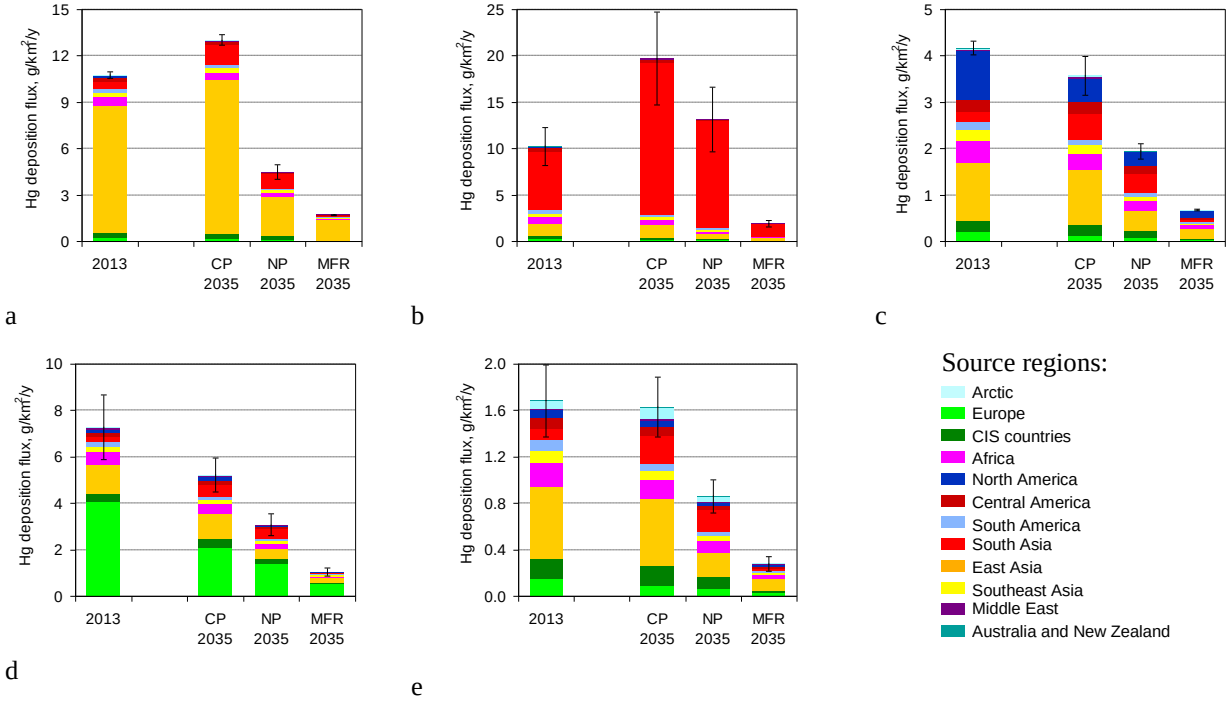

Fig. 14. Source apportionment of Hg deposition from direct anthropogenic sources (average of two models) in 2013 and 2035 in various geographical regions: (a) – East Asia; (b) – South America; (c) – North America a; (d) – Europe; (e) – Arctic. Whiskers show deviation between the models. Note different scales of the diagrams for different regions.

Atmos. Chem. Phys. Discuss., doi:10.5194/acp-2016-370, 2016
Manuscript under review for journal Atmos. Chem. Phys.
Published: 25 May 2016

Atmospheric Chemistry and Physics Discussions

Annex A.

Table A.1. Location, network and coordinates of measurement sites used in model evaluation

Site, location	Network	Longitude	Latitude	Altitude [c]
Amsterdam Island, Indian Ocean	GMOS [a]	77.6	-37.8	70
Andøya, Norway	EMEP [b]	16.0	69.3	380
Bariloche, Argentina	GMOS	-71.4	-41.1	801
Birkenes, Norway	EMEP	8.3	58.4	219
Bredkälen, Sweden	EMEP	15.3	63.9	404
Calhau, Sao Vicente, Atlantic Ocean	GMOS	-24.9	16.9	10
Cape Point, South Africa	GMOS	18.5	-34.4	230
Diabla Gora, Poland	EMEP	22.1	54.2	157
Dome Concordia, Antarctica	GMOS	123.3	-75.1	3220
Ev-K2, Nepal	GMOS	86.8	28.0	5050
Kodaikanal, India	GMOS	77.5	10.2	2333
Listvyanka, Russia	GMOS	104.9	51.8	670
Longobucco, Italia	GMOS	16.6	39.4	1379
Mace Head, Ireland	EMEP	-9.9	53.3	15
Manaus, Brazil	GMOS	-60.0	-2.9	110
Mt. Ailao, China	GMOS	101.0	24.5	2503
Mt. Changbai, China	GMOS	128.1	42.4	741
Mt. Waliguan, China	GMOS	100.9	36.3	3816
Nieuw Nickerie, Surinam	GMOS	-57.0	6.0	1
Pallas, Finland	EMEP	24.2	68.0	340
Råö, Sweden	EMEP	11.9	57.4	5
Sisal, Yucatan, Mexico	GMOS	-90.0	21.2	7
Station Nord, Greenland, Denmark	EMEP	-16.6	81.6	30
Troll Research Station, Antarctica	EMEP	2.5	-72.0	1275
Vavihill, Sweden	EMEP	13.2	56.0	175
Waldhof, Germany	EMEP	10.8	52.8	74
Zeppelin, Spitsbergen, Norway	EMEP	11.9	78.9	474

[a] Global Mercury Observation System (GMOS), http://www.gmos.eu/sdi/
[b] EMEP monitoring network, http://ebas.nilu.no/
[c] Unit for altitude is meters.